State selection of molecular oxygen ($^3\Sigma_g^-$) by a hexapole magnet and the inversion of population for the spin-rotational states

Mitsunori Kurahashi and Yasushi Yamauchi
National Institute for Materials Science, 1-2-1 Sengen, Tsukuba, Ibaraki 305-0047, Japan
(Received 1 July 2008; published 13 August 2008)

State selection of molecular oxygen ($^3\Sigma_g^-$) by a hexapole magnet and the inversion of population for the O_2 spin-rotational states by a two-coil spin flipper are reported. The Stern-Gerlach magnetic deflection spectra of a supersonic O_2 beam which is passed through the hexapole magnet show peaks associated with the O_2 spin-rotational states with the magnetic quantum number $M_J \geqslant 0$. Peaks corresponding to the states with $M_J \leqslant 0$ appear when the beam is passed through an opposing magnetic field formed in the two-coil spin flipper. The present results indicate that a hexapole magnet can select the spin-rotational states of O_2 and the polarity of M_J can be reversed by the diabatic passage through an opposing magnetic field.

DOI: 10.1103/PhysRevA.78.022708 PACS number(s): 34.80.Nz, 33.20.Wr, 79.20.Rf

I. INTRODUCTION

Preparation of a spin-polarized neutral particle beam using a hexapole magnet has been reported for atomic species such as hydrogen [1], alkali atoms [2,3], and metastable rare gas atoms [4–7] for their applications in atomic, nuclear and surface physics. The same technique could also be used for the state selection of more complex and chemically interesting species to investigate the spin effect in chemical reactions. The application of this technique to molecular species is, however, very limited and the only experiment which we are aware of is that conducted for a NO molecular beam by Anderson *et al.* [8] In the present study, we have made an attempt to use a hexapole magnet for the state selection of the ground state triplet O_2 ($^3\Sigma_g^-$) molecule, which would be one of the most important chemical species in every field of natural science. In spite of the numerous studies conducted for various oxidation processes, little is known about the effect of O_2 spin. Spin effects of O_2 have attracted much attention recently since it was proposed by a theoretical calculation that the spin selection rule plays an important role in the oxidation of Al(111) surface [9]. No experimental evidences, however, have been reported that directly show the spin effect. A state-selected O_2 beam would be useful to study spin-dependent processes in various oxidation reactions.

So far, magnetic deflection of O_2 has been investigated by a couple of groups [10–13]. Because O_2 is a diatomic molecule, the spin magnetic moment derived from the two unpaired electrons couples with the angular momentum due to the nuclear rotation, giving rise to complex Zeeman splittings. To avoid the complex splittings due to the rotational motion, most of the magnetic deflection experiments have been conducted for an O_2 beam cooled by supersonic expansion [10–13]. Kuebler *et al.* [10] have shown that the Stern-Gerlach (SG) spectra for an unpolarized O_2 beam can be well explained by the Zeeman splittings calculated for the spin-rotational states of O_2. Aquilanti *et al.* [11,12] have reported the rotational alignment effect of the O_2 molecule by a supersonic expansion of the oxygen gas seeded with other gases. Fujisawa *et al.* [13] have reported the enhancement of the O_2 sheet beam intensity by using an inhomogeneous magnetic field. No attempts, however, have been made to produce a state-selected O_2 beam by using a hexapole magnet and conduct a beam polarization analysis.

The inversion of population for the spin states, which we will discuss for the molecular oxygen, has often been conducted to detect the difference between parallel and antiparallel spin configurations of a beam and a target. It is of great advantage experimentally if the beam polarization can be changed with a high repetition rate keeping the target polarization fixed. The spin flippers have been used for experiments with polarized particle beams for such purposes. The two-coil spin flipper [3–6,14–16] has been used for simple systems such as metastable hydrogen [14], neutron [15], alkali atoms [3], and metastable helium (He*) [4–6], but there has been no attempt to use it for flipping the magnetic quantum number (M_J) of a complex molecule.

In the present paper, we report the state selection of the ground state O_2 molecule by a hexapole magnet and the population inversion of the O_2 spin-rotational states by the two-coil spin flipper. It is shown that the SG spectra exhibit fine structures corresponding to the spin-rotational levels, and the spectra are changed substantially when the mode of the spin flipper is altered. This behavior can be associated with the polarity change of M_J. The present results indicate that we can select the spin-rotational states of O_2 by a hexapole magnet and reverse the polarity of M_J using a two-coil flipper.

II. EXPERIMENT

A. Beamline

Figure 1 shows the schematic diagram for the beamline. The basic structure of the beamline is the same as that used for our previous measurements for the spin-polarized metastable atom deexcitation spectroscopy [5,6]. Before studying the magnetic deflection of O_2, we conducted the SG analysis of a metastable helium (He*, 2^3S) beam using the same beamline for calibration of the magnetic deflection experiment. The He* atom was generated by continuous discharge as has been described in previous papers [17,18].

The O_2 source is a pulsed valve (General Valve Corporation) operating with a nozzle diameter of 50 μm and at stag-

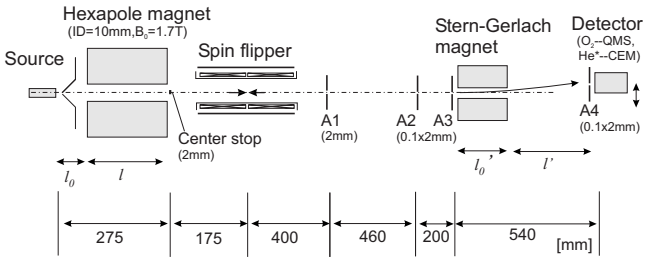

FIG. 1. Schematic diagram for the experimental apparatus.

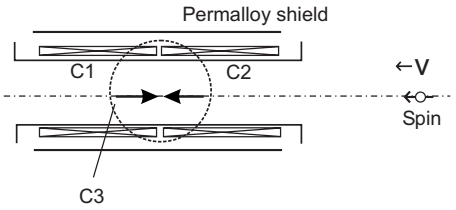

FIG. 2. Schematic diagram for the two-coil spin flipper.

nation pressures of 50–2000 Torr, but it was operated mostly in a continuous mode. The hexapole magnet is 180 mm long, 90 mm in diameter, and has a bore of 10 mm [5,6]. It is a Halbach type [20] and consists of Nd-Fe-B magnets. A central stop located at the exit of the hexapole magnet removes nonmagnetic species such as photons generated by He* discharge and He* (2^1S). The Stern-Gerlach magnet also consists of permanent magnets. He* and O_2 was detected with a channeltron and a quadrupole mass spectrometer, respectively. Both the channeltron and the mass spectrometer are mounted on a stage, the position of which can be scanned using a stepping motor.

B. Magnetic deflection in the hexapole magnet and the SG magnet

The inhomogeneous magnetic field in the pole gap of a hexapole magnet provide a force which is proportional to the atoms' radial distance r from the axis and directed towards the axis if the effective magnetic moment $(\mu_{eff})<0$, away from the axis if $\mu_{eff}>0$ [21]. The force $F(r)$ can be expressed as follows if μ_{eff} is field-independent [for the case of O_2, in which μ_{eff} depends on the field, Eqs. (1) and (2) should be used only for a qualitative discussion]:

$$F(r) = 2\mu_{eff}\frac{B_0}{r_0^2}r. \tag{1}$$

Here, r_0 is the bore radius and B_0 is the magnetic field at $r=r_0$. This deflection force causes a harmonic oscillation of a particle with $\mu_{eff}<0$ at the frequency $w=\sqrt{2|\mu_{eff}|B_0/(mr_0^2)}$, where m is the mass of the particle. In the present case, because the SG analyzer is largely separated from the hexapole magnet, a particle beam which have a high intensity at the entrance of the SG analyzer would be nearly parallel to the beamline at the exit of the hexapole magnet. The condition for this is as follows:

$$l\sqrt{\frac{B_0}{r_0^2}\frac{\mu_{eff}}{E_{kin}}} + \tan^{-1}\left(l_0\sqrt{\frac{B_0}{r_0^2}\frac{\mu_{eff}}{E_{kin}}}\right) = \frac{\pi}{2} \tag{2}$$

Here, E_{kin}, l, and l_0 are the particle's kinetic energy along the beamline, the length of the hexapole magnet and the distance from the nozzle to the hexapole entrance, respectively (see Fig. 1). It is noted that Eq. (2) depends only on the ratio μ_{eff}/E_{kin}.

The SG analysis has been made with a magnet having a pair of concave and convex hemicylindrical pole pieces of different radii. It is well known that the field in the gap of this type of magnet is given by the two-wire model [21]. The deflection (d) of a particle with μ_{eff} and E_{kin} is given by

$$d = \frac{\mu_{eff}(\nabla B)}{E_{kin}}\left(\frac{1}{2}l'l_0' + \frac{1}{4}l_0'^2\right), \tag{3}$$

where l_0' and l' are the length of the SG magnet and the distance from the exit of the SG magnet to the detector, respectively (see Fig. 1). Similar to the case of Eq. (2), the deflection is determined by the ratio μ_{eff}/E_{kin}. In the case of the SG experiment, the field seen by the particle would not change largely during the passage in the SG magnet because the deflection in the SG magnet is so small. Equation (3) would therefore be applicable also to O_2 although μ_{eff} of O_2 depends on the field. Here, the magnetic field averaged along the flight path in the SG magnet was estimated to be 0.8 T from the SG deflection of He* (2^3S).

C. Spin flipper

A spin flipper that has been used for flipping the spin polarization of the He* beam [4–6] was used for reversing the polarity of M_J of O_2. The schematic diagram of the flipper is shown in Fig. 2. The flipper consists of two coils $(C1, C2)$ that are placed in series and generate an opposing magnetic field, a coil for generating a transverse field $(C3)$ and a permalloy shield [5]. When a particle passes through the flipper, it feels a time-varying magnetic field. When $C3$ is off (on), the field direction seen by the particle changes suddenly (gradually) at the flipping point. Here, because the field is very weak at the flipping point, the total angular momentum J is a good quantum number during the passage [3,16]. Since the field is time-varying, transitions among magnetic sublevels can occur [16]. If the field changes slowly compared to the Larmor precession frequency ω_L, the initial state $|J,M_J\rangle$ defined with respect to the initial field changes into the corresponding final state $|J,M_J\rangle$ in the final field seen by the particle [16,22]. In this case, M_J does not change (adiabatic case). In contrast, if the field changes rapidly compared to ω_L, the initial state $|J,M_J\rangle$ defined with respect to the initial field remains in the same state, which can be described as a superposition of several states $|J,M_J'\rangle$ in the final field seen by the particle at a later time [16,22]. If the field reverses, the initial state $|J,M_J\rangle$ is changed to $|J,-M_J\rangle$ after the passage (diabatic case).

To realize the diabatic passage, the sign of the field seen by the beam has to be changed in a short time compared to ω_L. The time for the field reversal is inversely proportional to the particle velocity. In the present experiment, as will be shown later, the velocity of He* and O_2 are ~2700 m/s and

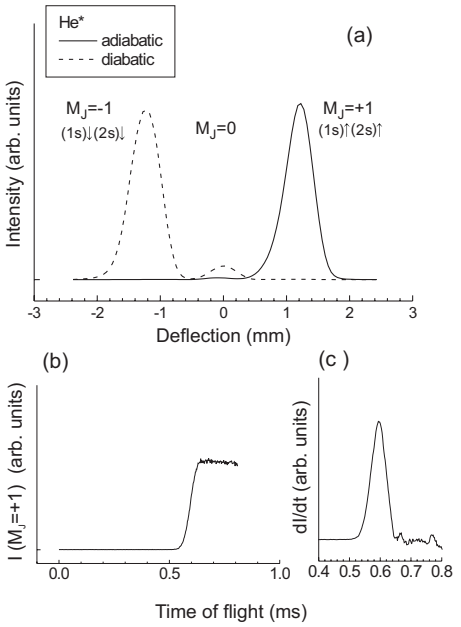

FIG. 3. (a) The Stern-Gerlach spectrum for He* (2^3S) atoms measured for the adiabatic (solid line) and diabatic (dashed line) cases in the flipper. (b) The time resolved intensity measured at the deflection of 1.2 mm, which corresponds to the peak position of $M_J=+1$, when switching the flipper mode. $t=0$ corresponds to the time when the flipper mode is changed to the adiabatic mode. The onset corresponds to the flight time of He* from the flipper to the SG detector ($L=1.6$ m). The numerical derivative of the TOF spectra (b) is shown in (c).

$\sim$750 m/s, respectively, while the value of ω_L would be similar because they have similar μ_{eff} values. For realizing the diabatic passage for O_2, therefore, the magnetic field direction should change in a shorter distance at the flipping point. In this sense, the condition for the opposing field necessary for the diabatic passage is more stringent for O_2. The spin flipping efficiency of the O_2 beam would therefore be lower than the He* beam if the same flipper (opposing field) is used. As will be shown later, however, the SG spectra for the O_2 beam exhibit a substantial change, indicating that the diabatic passage is dominant also for the O_2 case.

D. SG analysis of the He* beam

Figure 3 shows the SG spectra measured for the He* beam. When the flipper is in the adiabatic mode ($C3$ is on), only one peak corresponding to $M_J=+1[(1s)_\uparrow(2s)_\uparrow]$ appears, indicating that the beam coming out from the hexapole magnet is almost 100% spin polarized. For the case of the diabatic passage ($C3$ is off), the $M_J=+1$ peak disappears almost completely, and a dominant peak due to $M_J=-1$ emerges, indicating a high spin flipping efficiency. A small peak for the $M_J=0$ component is due to the incomplete spin flip, which may be caused by the nonzero radial field component at the flipping point [3–6].

We note the following as to the depolarizing (Majorana) transitions [16] outside the spin flipper. If the magnetic field changes within a short distance at some positions on the beamline, the beam depolarization may occur. The depolarization is caused by the diabatic process [16] discussed in Sec. II C. The present He* SG analysis for the adiabatic case, which shows the beam polarization of $\sim$100%, indicates that no depolarizing transition occurs for He* after the He* beam passes through the hexapole magnet. From this, we can deduce that no depolarizing transition would occur for the O_2 beam. This is because, as has been discussed in Sec. II C, the diabatic condition is more difficult to be realized for the O_2 beam than the He* beam because the O_2 molecules are slower.

Figure 3(b) shows the time-resolved intensity monitored at the $M_J=+1$ peak position when switching the flipper mode. Here, $t=0$ corresponds to the time when the flipper mode is changed to the adiabatic mode. Since the time delay reflects the particle velocity, we can evaluate the He* velocity from the position of the onset. Figure 3(c) shows the derivative of the He* intensity. From the position and width of the peak in the derivative spectrum, we can evaluate the He* velocity to be 2710 ± 150 m/s. We note that the He* atoms generated by the discharge source has a broad Maxwellian velocity distribution. The narrow peak width observed here, which corresponds to the energy spread of 0.036 eV, reflects the transmission characteristics of the hexapole magnet and defining apertures.

III. RESULTS

Figure 4 shows the SG spectra for the O_2 molecular beam measured at various stagnation pressures (P_S). The SG spectra show the following features. First, the spectra show a substantial change when the mode of the spin flipper is changed. Especially in the spectra taken at $P_S=1900$ Torr, the main peak at $d\sim+1.3$ mm in the adiabatic mode becomes almost quenched when the flipper mode is changed to the diabatic mode. This demonstrates that the diabatic passage becomes dominant in the present flipper also for the O_2 case. Second, the spectra depend on P_S. This P_S dependence would reflect the rotational temperature (T_{rot}) dependence of the O_2 molecule. Since it has been reported that $T_{rot}=4-6$ K at $P_S=460$ Torr for a 50 μm nozzle beam [19], the lowest rotational states should be dominant at $P_S>1000$ Torr. Third, the SG spectra show peaks at positions similar to the SG spectra of He*, but several peaks ($A-F$) are clearly seen. The position and intensity of these peaks depend on P_S.

Figures 5(a) and 5(b) show the time of flight (TOF) spectra taken at different SG deflection peak positions. The onset positions in Fig. 5(a) reflect the velocity of O_2 molecules that contribute to the SG peaks indicated. The TOF peak position can be seen more clearly in the derivative spectra shown in Fig. 5(b). These spectra show peaks at 2.0–2.4 ms, which correspond to the O_2 velocity of 800–670 m/s. This velocity range is consistent with the velocity reported for the O_2 beam generated by a supersonic expansion of a room temperature O_2 gas. [10,13] Note that the position of the TOF peaks (D', E', A', and A'') differs depending on the SG deflection peak positions. The velocities of the species associated with D' and E' are 800 m/s and 670 m/s, respectively. There are

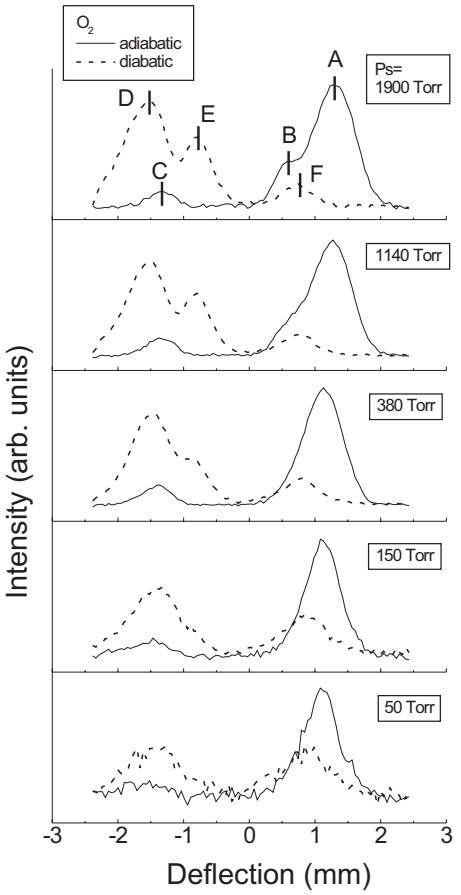

FIG. 4. The Stern-Gerlach spectra measured for the O_2 molecular beam at the stagnation pressures (P_S) shown.

two components (A' and A'') for the SG peak A, and their positions are close to peaks D' and E', respectively. This indicates that the species associated with A' and D' are identical before passing through the spin flipper, and the same is true for A'' and E'. The O_2 species with different velocities can contribute to the SG spectra if the ratio μ_{eff}/E_{kin} satisfies Eq. (3). The species with lower (higher) velocity would correspond to those with smaller (larger) μ_{eff}.

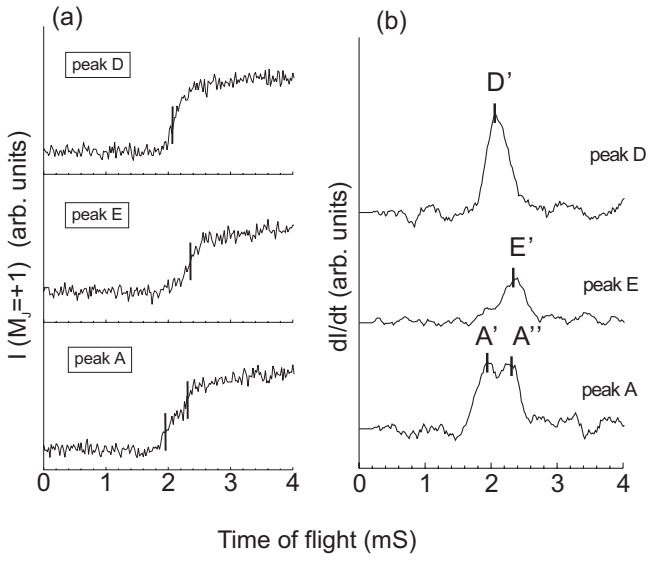

FIG. 5. (a) The TOF spectra measured for the O_2 beam with P_S=1140 Torr at the SG peak positions indicated in Fig. 4. Corresponding derivative spectra are shown in (b).

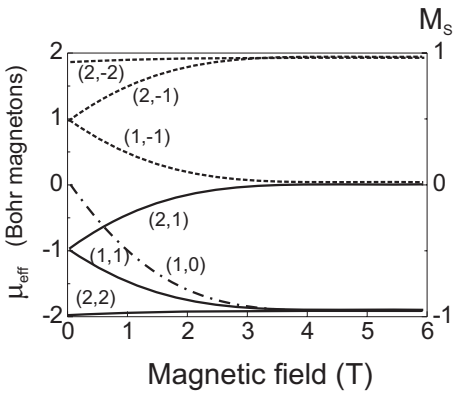

FIG. 6. An illustration of the magnetic field dependence of the effective magnetic moment for the O_2 spin-rotational states calculated by Aquilanti *et al.* [11]. The J and M_J values indicated are for those for corresponding levels. The curves are shown only for those levels which can contribute to the present SG spectra. The states responsible for the SG spectra of the adiabatic (diabatic) case are shown with solid (broken) lines. The (1,0) state would contribute to both cases as noted in the text.

IV. DISCUSSIONS

The origin of the SG peaks is discussed below on the basis of Zeeman energies of O_2. Because T_{rot} would be <4 K at $P_S>1000$ Torr as has been noted before, most of the molecules would be in the lowest rotational states. Because the rotational levels with $K=0,2,4,\ldots$ are not allowed in $^{16}O_2$ as a consequence of the nuclear statistics, the lowest rotational level is $K=1$ in $^{16}O_2$ [10]. The rotational angular momentum K in O_2 is added vectorically to the spin angular momentum $S=1$ to generate the angular momentum vector $J=K+S$, which equals 0, 1, and 2 when $K=1$. It has been expected that there is a thermal equilibrium among the three J levels of $K=1$ in the molecular beam [10]. Each J component has $2J+1$ sublevels, each with a characteristic Zeeman energy in a magnetic field.

Figure 6 illustrates the magnetic field dependence of the effective magnetic moments, which have been calculated as $\mu_{eff}=-dE/dH$ by Aquilanti *et al.* [11], for the $J=0,1,2$ levels derived from $K=1$. The curves are shown only for those levels which may contribute to the present SG spectra. For discussing the peak positions of the SG spectra, we should use the μ_{eff} values at 0.8 T, which is the field seen by the O_2 molecules in the SG magnet as noted in Sec. II D.

We note the following as to the effective magnetic moment in the hexapole magnet. If the particle has a field-independent effective magnetic moment, the hexapole magnet transmits those species for which the ratio μ_{eff}/E_{kin} satisfies Eq. (2). Following Eq. (3), all of the species with the μ_{eff}/E_{kin} value resulting from Eq. (2) should give rise to the same SG deflection. However, the present SG spectra exhibit multiple peak structures. There are two reasons for this. One

TABLE I. The Stern-Gerlach deflection for the adiabatic mode. The deflection for each levels has been estimated using the measured O_2 velocities and the μ_{eff} values obtained from Ref. [11].

(J, M_J)	μ_{eff} (μ_B)	v_{O_2} (m/s)	deflection (mm)	assignment
(2,2)	−1.9	800	1.6	*A*
(1,1)	−1.3	670	1.6	*A*
(1,0)	−0.8	<670	>1.0	*B*(*F*)
(2,1)	−0.6	<670	>0.7	*B*

is that the μ_{eff} values depend on the field and the μ_{eff} values in the hexapole magnet are different from those in the SG magnet. The magnetic field in the hexapole magnet is 0–1.7 T depending on the radial distance from the axis. The other reason is that, as will be discussed in Sec. IV B, the magnitude of μ_{eff} is altered when the polarity of M_J is changed by the flipper.

A. Adiabatic mode

To discuss the SG peaks observed for the adiabatic mode, we should consider those states with $\mu_{eff}<0$ because the species with $\mu_{eff}>0$ are defocused by the hexapole magnet. Thus, the four states (2,2), (1,1), (1,0), and (2,1) can contribute to the SG spectra for the adiabatic mode. The μ_{eff} values obtained graphically from those calculated by Aquilanti *et al.* [11] are listed in Table I. Our TOF spectra [Fig. 5(b)] taken at peak *A*, the main peak for the adiabatic case, have two velocity components. If we assign A' and A'' to the (2,2) and (1,1) levels, respectively, the SG deflection is calculated with Eq. (3) to be ~1.6 mm, which is close to the position of peak *A*.

The SG spectra show a shoulder (peak *B*). Since the TOF analysis for peak *B* was difficult to conduct, the velocity of the corresponding species is unknown. Since $|\mu_{eff}|$ for (1,0) and (2,1) states is less than that for (1,1) over all field ranges as shown in Fig. 6, the velocity of these species would be less than 670 m/s, and the deflections are roughly estimated (see Table I).

B. Diabatic mode

The polarity of M_J is expected to flip by the diabatic passage through an opposing field as has been discussed in Sec. II C. Therefore, the polarity of M_J for the four O_2 species which pass through the hexapole magnet would flip as shown in Table II. Here, the velocity of the species does not change before and after passing the flipper. The SG deflections calculated using the μ_{eff} values obtained from Ref. [11] are also listed in Table II. The deflection calculated for (2,−2) agree well with the position of peak *D*. It is interesting that the magnitude of μ_{eff} for (1,1) decreases to $0.6\mu_B$ after the transition to (1,−1). The corresponding deflection is expected to become smaller as shown in Table II. This deflection agrees well with that for peak *E*. As to the (1,0) states, because $M_J=0$, the peak should remain unchanged when switching the mode of the flipper. Actually, a peak remains at $d\sim0.8$ mm (peak *F*), which can be attributed to the (1,0) state. This is also consistent with the presence of the shoulder (peak *B*) for the adiabatic case. The magnitude of μ_{eff} for the (2,1) state increases after the transition to (2,−1). The (2,−1) state would contribute to peak *D*. The intensity of the (2,−1) state, as can be expected from the intensity of peak *B*, is so small that the TOF spectra taken at peak *D* would not show the structure corresponding to the (2,−1) state.

TABLE II. The Stern-Gerlach deflection for the diabatic mode.

(J, M_J)	μ_{eff} (μ_B)	v_{O_2} (m/s)	deflection (mm)	assignment
(2,−2)	+1.9	800	−1.6	*D*
(1,−1)	+0.6	670	−0.7	*E*
(1,0)	−0.8	<670	>1.0	*F*(*B*)
(2,−1)	+1.3	<670	<−1.6	*D*

The SG spectra for the He* beam [Fig. 3(a)] show a peak caused by the incomplete spin flip ($M_J=0$). This incomplete spin flip is because a perfectly diabatic passage is not realized mainly due to the nonzero radial component of the magnetic field as mentioned in Sec. II D. This nonzero radial component causes a transition to $M\rightarrow M\pm1$ [3]. As noted in Sec. II D, the flipping efficiency would be lower for O_2. Transitions like $(2,2)\rightarrow(2,1)$, $(1,1)\rightarrow(1,0)$ are therefore possible to occur. The corresponding peaks are however not visible because they overlap with a peak at around $d\sim0.8$ mm (peak *F*).

C. Stagnation pressure dependence of the SG spectra

The SG spectra depend considerably on P_S as shown in Fig. 5. The major change with the decrease in P_S is that the relative intensity of peak *E* decreases and that of peak *F* increases. This would be caused by the increase of T_{rot} with the decrease in P_S. The levels that are derived from $K>1$ should be considered for discussing the P_S dependence of the SG spectra.

The change in the SG spectra with P_S may be associated with the difference between the $J=1$ and $J=3$ levels, which are derived from $K=1$ and $K=3$, respectively. There are three magnetic sublevels for $J=1$. At the Paschen-Back (high field) limit, two of the three sublevels [(1,1) and (1,0)] are bundled into $M_S=+1$, and therefore μ_{eff} increases and approaches to $2\mu_B$ with increasing *H* (see Fig. 6) [10,11]. However, because the (1,−1) state converges to $M_S=0$ at high fields [10,11], $|\mu_{eff}|$ for the (1,−1) state decreases with *H*. This causes the difference in $|\mu_{eff}|$ between (1,1) and (1,−1). Because of the smaller $|\mu_{eff}|$ for (1,−1) than (1,1), a SG peak with a smaller deflection (peak *E*) appears. As to the $J=3$ levels, there are seven magnetic sublevels. At the high field limit, only (3,−3) converges to $M_S=0$ level, and the other six levels are bundled into $M_S=+1$ [10]. Therefore, the following situation is expected. When changing the flipper mode to the diabatic mode, the (3,3) state would be changed into the (3,−3) state, possibly giving rise to a SG deflection peak such as peak *E*. However, even if the (3,2), (3,1), (3,0),

$(3,-1)$, and $(3,-2)$ states, which can pass through the hexapole magnet, changes M_J values, the polarity of μ_{eff} does not change and the SG peak does not shift to negative deflection side. Thus we can expect that, when the flipper mode is changed, the $(3,-2)$, $(3,-1)$, (3,0), (3,1), and (3,2) states give rise to peaks at the positive deflection side and only the $(3,-3)$ state would result in a peak at the negative deflection side. This is consistent with the observation that the relative intensity of the peak on the positive deflection side becomes high and the peak at $d \sim -0.7$ mm decays with the decrease of P_S.

D. The origin of peak *C*

The origin of peak *C* is not clear at present. Peak *C* exists even at high P_S, and its intensity relative to peak *A* does not change largely with P_S. We have also confirmed that this peak is not derived from the background O_2 gas because the peak disappears if the beam is cut by locating a small plate in the beamline. The velocity of the corresponding species was measured by pulsing the valve and found to be about 630 m/s.

One of the possible origin is the effect of the avoided crossings. The levels derived from the $K=3$ manifold show some avoided crossings at low field region [10,23]. The energy vs H curve changes the polarity of the slope before and after the crossings, causing the polarity change in μ_{eff} [10,23]. As noted above, the magnetic field seen by the O_2 molecule in the hexapole magnet, which is 0–1.7 T depending on the radial distance from the axis, is different from that in the SG magnet. It is therefore possible that the species, although they have negative μ_{eff} in the hexapole magnet, have positive μ_{eff} in the SG magnet, causing an SG peak in the negative deflection side. However, the contribution of $K=3$ derived levels should depend on T_{rot} while the relative intensity of peak *C* is insensitive to P_S. For further discussions, a series of SG analysis for the O_2 beam with different velocities will be helpful.

V. CONCLUSIONS

Based on the Stern-Gerlach analysis of a supersonic O_2 beam, we have shown that a hexapole magnet can select the O_2 spin-rotational states and the polarity of M_J can be flipped by the diabatic passage through an opposing field. Considering the fact that each O_2 species has different μ_{eff} and the hexapole magnet transmits species with a given μ_{eff}/E_{kin} value, we will be able to select each O_2 species more precisely by tuning the O_2 velocity and improving the Mach number of the supersonic beam.

ACKNOWLEDGMENT

We are grateful to Dr. M. Yata for stimulating discussions.

[1] T. Wise, A. D. Roberts, and W. Haeberli, Nucl. Instrum. Methods Phys. Res. A **336**, 410 (1993), and references therein.
[2] V. W. Hughes, R. L. Long, Jr., M. S. Lubell, M. Posner, and W. Raith, Phys. Rev. A **5**, 195 (1972).
[3] W. Schröder and G. Baum, J. Phys. E **16**, 52 (1983).
[4] G. Baum, W. Raith, and H. Steidl, Z. Phys. D: At., Mol. Clusters **10**, 171 (1988).
[5] Y. Yamauchi, M. Kurahashi, T. Suzuki, and G. L. Gong, in Proceedings of 10th International Symposium on Advanced Physical Fields, 2005 (unpublished), p. 435.
[6] M. Kurahashi and Y. Yamauchi, Rev. Sci. Instrum. **79**, 073902 (2008).
[7] D. Watanabe, H. Ohoyama, T. Matsumura, and T. Kasai, Phys. Rev. Lett. **99**, 043201 (2007).
[8] S. L. Anderson, P. R. Brooks, J. D. Fite, and O. V. Nguyen, J. Chem. Phys. **72**, 6521 (1980).
[9] J. Behler, B. Delley, S. Lorenz, K. Reuter, and M. Scheffler, Phys. Rev. Lett. **94**, 036104 (2005).
[10] N. A. Kuebler, M. B. Robin, J. J. Yang, A. Gedanken, and D. R. Herrick, Phys. Rev. A **38**, 737 (1988).
[11] V. Aquilanti, D. Ascenzi, D. Cappelletti, and F. Pirani, J. Phys. Chem. **99**, 13620 (1995).
[12] V. Aquilanti, D. Ascenzi, D. Cappelletti, and F. Pirani, Nature (London) **371**, 399 (1994).
[13] T. Fujisawa, Y. Hashimoto, T. Morimoto, and Y. Fujita, Nucl. Instrum. Methods Phys. Res. A **506**, 50 (2003).
[14] R. D. Hight and R. T. Robiscoe, Phys. Rev. A **17**, 561 (1978); **15**, 1079 (1977).
[15] P. Liaud, R. I. Steinberg, and B. Vignon, Nucl. Instrum. Methods **125**, 7 (1975).
[16] S. Iannotta, in *Atomic and Molecular Beam Methods*, edited by G. Scoles (Oxford University Press, New York, 1988), Vol. I.
[17] Y. Yamauchi and M. Kurahashi, Appl. Surf. Sci. **169-170**, 236 (2001).
[18] M. Kurahashi, T. Suzuki, X. Ju, and Y. Yamauchi, Phys. Rev. B **67**, 024407 (2003).
[19] T. Matsumoto and K. Kuwata, Chem. Phys. Lett. **171**, 314 (1990).
[20] K. Halbach, Nucl. Instrum. Methods **169**, 1 (1980).
[21] J. Reuss, in *Atomic and Molecular Beam Methods* (Ref. [16]).
[22] A. Messiah, *Quantum Mechanics* (North-Holland, Amsterdam, 1999).
[23] V. Aquilanti, D. Ascenzi, D. Cappelletti, and F. Pirani, Int. J. Mass Spectrom. Ion Process. **149**, 355 (1995).